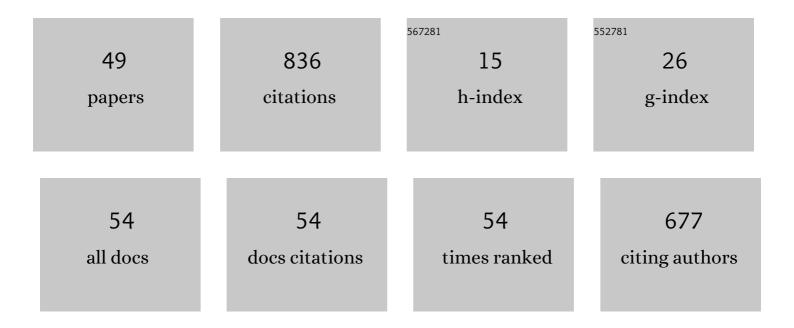
## Chengwu Huang

List of Publications by Year in descending order

Source: https://exaly.com/author-pdf/7537805/publications.pdf Version: 2024-02-01



#	Article	IF	CITATIONS
1	Quantitative Shear Wave Speed Assessment for Muscles With the Diagnosis of Taut Bands and/or Myofascial Trigger Points Using Probe Oscillation Shear Wave Elastography: A Pilot Study. Journal of Ultrasound in Medicine, 2022, 41, 845-854.	1.7	6
2	Super-Resolution Ultrasound Localization Microscopy for Visualization of the Ocular Blood Flow. IEEE Transactions on Biomedical Engineering, 2022, 69, 1585-1594.	4.2	14
3	Reverberation clutter signal suppression in ultrasound attenuation estimation using wavelet-based robust principal component analysis. Physics in Medicine and Biology, 2022, , .	3.0	0
4	In vivo assessment of hypertensive nephrosclerosis using ultrasound localization microscopy. Medical Physics, 2022, 49, 2295-2308.	3.0	16
5	Fast super-resolution ultrasound microvessel imaging using spatiotemporal data with deep fully convolutional neural network. Physics in Medicine and Biology, 2021, 66, 075005.	3.0	20
6	Improved Ultrasound Microvessel Imaging Using Deconvolution with Total Variation Regularization. Ultrasound in Medicine and Biology, 2021, 47, 1089-1098.	1.5	6
7	Super-resolution ultrasound localization microscopy based on a high frame-rate clinical ultrasound scanner: an in-human feasibility study. Physics in Medicine and Biology, 2021, 66, 08NT01.	3.0	61
8	Morphological Reconstruction Improves Microvessel Mapping in Super-Resolution Ultrasound. IEEE Transactions on Ultrasonics, Ferroelectrics, and Frequency Control, 2021, 68, 2141-2149.	3.0	7
9	Simultaneous Noise Suppression and Incoherent Artifact Reduction in Ultrafast Ultrasound Vascular Imaging. IEEE Transactions on Ultrasonics, Ferroelectrics, and Frequency Control, 2021, 68, 2075-2085.	3.0	19
10	Noise Suppression for Ultrasound Attenuation Coefficient Estimation Based on Spectrum Normalization. IEEE Transactions on Ultrasonics, Ferroelectrics, and Frequency Control, 2021, 68, 2667-2674.	3.0	4
11	Liraglutide reduces attenuation coefficient as a measure of hepatic steatosis during 16 weeks' treatment in nondiabetic obese patients: A pilot trial. JGH Open, 2021, 5, 193-198.	1.6	6
12	Localization of High-concentration Microbubbles for Ultrasound Localization Microscopy by Self-Supervised Deep Learning. , 2021, , .		6
13	In vivo Visualization of Pig Vagus Nerve "Vagotopy―Using Ultrasound. Frontiers in Neuroscience, 2021, 15, 676680.	2.8	9
14	Three-dimensional shear wave elastography on conventional ultrasound scanners with external vibration. Physics in Medicine and Biology, 2020, 65, 215009.	3.0	9
15	Ultrasound Attenuation Estimation in Harmonic Imaging for Robust Fatty Liver Detection. Ultrasound in Medicine and Biology, 2020, 46, 3080-3087.	1.5	10
16	Changes in spinal cord hemodynamics reflect modulation of spinal network with different parameters of epidural stimulation. NeuroImage, 2020, 221, 117183.	4.2	16
17	Deep Variational Network for High Quality 3D Ultrasound Imaging using Sparse Array. , 2020, , .		1
18	445 LIRAGLUTIDE ESCALATED TO 3.0 MG REDUCES HEPATIC STEATOSIS DURING 16 WEEKS' TREATMENT IN NON-DIABETIC OBESE PATIENTS. Gastroenterology, 2020, 158, S-86.	1.3	0

CHENGWU HUANG

#	Article	IF	CITATIONS
19	Ultrasound localization microscopy of renal tumor xenografts in chicken embryo is correlated to hypoxia. Scientific Reports, 2020, 10, 2478.	3.3	53
20	Real time SVD-based clutter filtering using randomized singular value decomposition and spatial downsampling for micro-vessel imaging on a Verasonics ultrasound system. Ultrasonics, 2020, 107, 106163.	3.9	38
21	Short Acquisition Time Super-Resolution Ultrasound Microvessel Imaging via Microbubble Separation. Scientific Reports, 2020, 10, 6007.	3.3	67
22	Kalman Filter-Based Microbubble Tracking for Robust Super-Resolution Ultrasound Microvessel Imaging. IEEE Transactions on Ultrasonics, Ferroelectrics, and Frequency Control, 2020, 67, 1738-1751.	3.0	70
23	<i>In Vivo</i> Confocal Imaging of Fluorescently Labeled Microbubbles: Implications for Ultrasound Localization Microscopy. IEEE Transactions on Ultrasonics, Ferroelectrics, and Frequency Control, 2020, 67, 1811-1819.	3.0	20
24	Quantitative Inflammation Assessment for Crohn Disease Using Ultrasensitive Ultrasound Microvessel Imaging. Journal of Ultrasound in Medicine, 2020, 39, 1819-1827.	1.7	4
25	Multi-resolution Data Processing for Accelerated and Robust Ultrasound Localization Microscopy. , 2020, , .		0
26	Ultrasonographic findings of intrahepatic lymphoepithelioma-like cholangiocarcinoma associated with Epstein–Barr virus. Medicine (United States), 2019, 98, e14206.	1.0	13
27	Debiasing-Based Noise Suppression for Ultrafast Ultrasound Microvessel Imaging. IEEE Transactions on Ultrasonics, Ferroelectrics, and Frequency Control, 2019, 66, 1281-1291.	3.0	37
28	System-Independent Ultrasound Attenuation Coefficient Estimation Using Spectra Normalization. IEEE Transactions on Ultrasonics, Ferroelectrics, and Frequency Control, 2019, 66, 867-875.	3.0	19
29	Noninvasive Contrast-Free 3D Evaluation of Tumor Angiogenesis with Ultrasensitive Ultrasound Microvessel Imaging. Scientific Reports, 2019, 9, 4907.	3.3	30
30	Functional Ultrasound Imaging of Spinal Cord Hemodynamic Responses to Epidural Electrical Stimulation: A Feasibility Study. Frontiers in Neurology, 2019, 10, 279.	2.4	38
31	Pulse Wave Imaging for Assessing Arterial Stiffness Change in A Mouse Model of Thoracic Aortic Dissection in Marfan Syndrome. , 2019, , .		1
32	Ultrasensitive Ultrasound Microvessel Imaging for Characterizing Benign and Malignant Breast Tumors. Ultrasound in Medicine and Biology, 2019, 45, 3128-3136.	1.5	14
33	Three-dimensional Super-Resolution Ultrasound Microvessel Imaging with Bipartite Graph-based Microbubble Tracking using a Verasonics 256-channel Ultrasound System. , 2019, , .		2
34	Interoperator Reproducibility of Carotid Elastography for Identification of Vulnerable Atherosclerotic Plaques. IEEE Transactions on Ultrasonics, Ferroelectrics, and Frequency Control, 2019, 66, 505-516.	3.0	15
35	On Combination of Hadamard-Encoded Multipulses and Multiplane Wave Transmission in Contrast-Enhanced Ultrasound Imaging. IEEE Transactions on Ultrasonics, Ferroelectrics, and Frequency Control, 2018, 65, 1977-1980.	3.0	2
36	A net-shaped multicellular formation facilitates the maturation of hPSC-derived cardiomyocytes through mechanical and electrophysiological stimuli. Aging, 2018, 10, 532-548.	3.1	6

Chengwu Huang

#	Article	IF	CITATIONS
37	Non-Invasive Identification of Vulnerable Atherosclerotic Plaques Using Texture Analysis in Ultrasound Carotid Elastography: An InÂVivo Feasibility Study Validated by Magnetic Resonance Imaging. Ultrasound in Medicine and Biology, 2017, 43, 817-830.	1.5	25
38	A Systematic Investigation of Lateral Estimation Using Various Interpolation Approaches in Conventional Ultrasound Imaging. IEEE Transactions on Ultrasonics, Ferroelectrics, and Frequency Control, 2017, 64, 1149-1160.	3.0	25
39	Notice of Removal: Suppression of reflected waves with high-resolution Radon transform for accurate measurement of regional pulse wave velocity. , 2017, , .		Ο
40	Noninvasive measurement of regional pulse wave velocity in human ascending aorta with ultrasound imaging. Journal of Hypertension, 2016, 34, 2026-2037.	0.5	13
41	High frame rate and high line density ultrasound imaging for local pulse wave velocity estimation using motion matching: A feasibility study on vessel phantoms. Ultrasonics, 2016, 67, 41-54.	3.9	12
42	Comparison of Different Pulse Waveforms for Local Pulse Wave Velocity Measurement in Healthy and Hypertensive Common Carotid Arteries inÂVivo. Ultrasound in Medicine and Biology, 2016, 42, 1111-1123.	1.5	23
43	Ultrasound-Based Carotid Elastography for Detection ofÂVulnerable Atherosclerotic Plaques Validated by MagneticÂResonance Imaging. Ultrasound in Medicine and Biology, 2016, 42, 365-377.	1.5	61
44	High line-density pulse wave imaging for local pulse wave velocity estimation using motion matching: A feasibility study on vessel phantoms. , 2015, , .		0
45	Pulse wave velocity measurement in healthy and diseased carotid arteries in vivo. , 2015, , .		Ο
46	Wide-angle tissue Doppler imaging at high frame rate using multi-line transmit beamforming: An in-vivo pilot study. , 2014, , .		1
47	Effects of key parameters on the performance of local pulse wave velocity measurement: Theroretial analysis and in-vivo validation. , 2014, , .		1
48	Effects of key parameters on the accuracy and precision of local pulse wave velocity measurement by ultrasound imaging. , 2014, 2014, 2877-80.		2
49	Effects of parameters on the accuracy and precision of ultrasound-based local pulse wave velocity measurement: a simulation study. IEEE Transactions on Ultrasonics, Ferroelectrics, and Frequency Control, 2014, 61, 2001-2018.	3.0	21